Galaxies, Cosmology and Dark Matter

Lecture given by
Ralf Bender
USM

Script by:
Christine Botzler, Armin Gabasch,
Georg Feulner, Jan Snigula

Summer semester 2000

Chapter 6

Dwarf Galaxies

6.1 Overview

Dwarf galaxies are usually divided into two classes:

1. **Dwarf ellipticals (dE)**, or **dwarf spheroidals (dSph)**:
   - morphologically similar to bright ellipticals
   - smooth surface brightness distributions
   - similar ellipticity distribution as bright ellipticals ($\rightarrow$ similar 3D shape)
   - no young stars
   - from bright to faint objects, surface brightness profiles show transition from $r^{1/4}$ profile (i.e. like bright ellipticals) to exponential profile (i.e. like disks)
   - surface brightnesses decline with decreasing luminosity, radii do not change much with luminosity ($r_e \sim$ 0.1 kpc - 1 kpc).

Elliptical Dwarf Galaxies (in Virgo cluster):

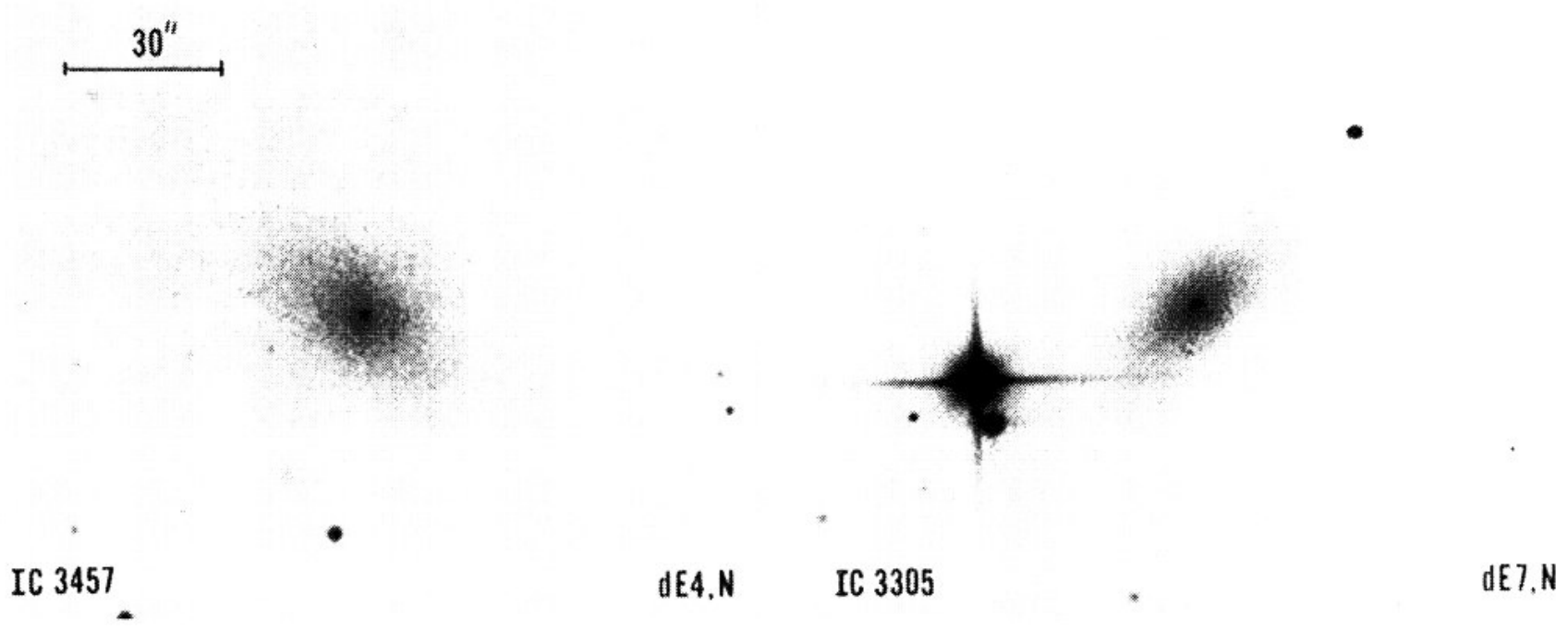

see: Sandage A., Binggeli B. (1984) *AJ*, **89**, 919

Distribution of Axial Ratios:

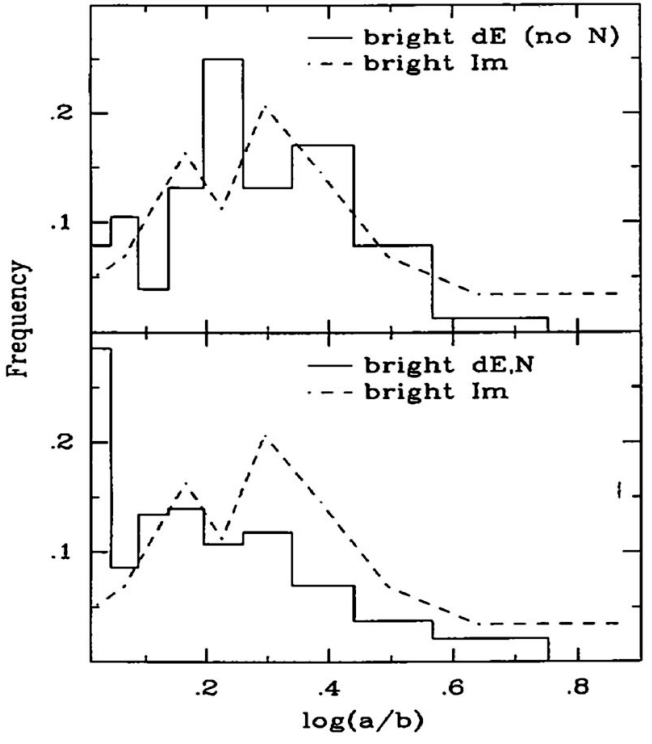

FIG. 3.—The distribution of axial ratios for bright nucleated and nonnucleated dE galaxies, and dwarf irregulars. The samples include likely members of the Virgo and Fornax Clusters brighter than $M_{B_T} = -14.7$. The Im sample includes 117 Sd, Sdm, Sm, and Im galaxies. The dE, N sample includes 186 galaxies, and the nonnucleated dE sample includes 79 galaxies. The bins in axial ratio are those used by Sandage, Freeman, and Stokes (1970).

see: Ferguson, Sandage (1989) *ApJ*, **346**, L53

Surface Brightness and Radius vs. Absolute Magnitude:

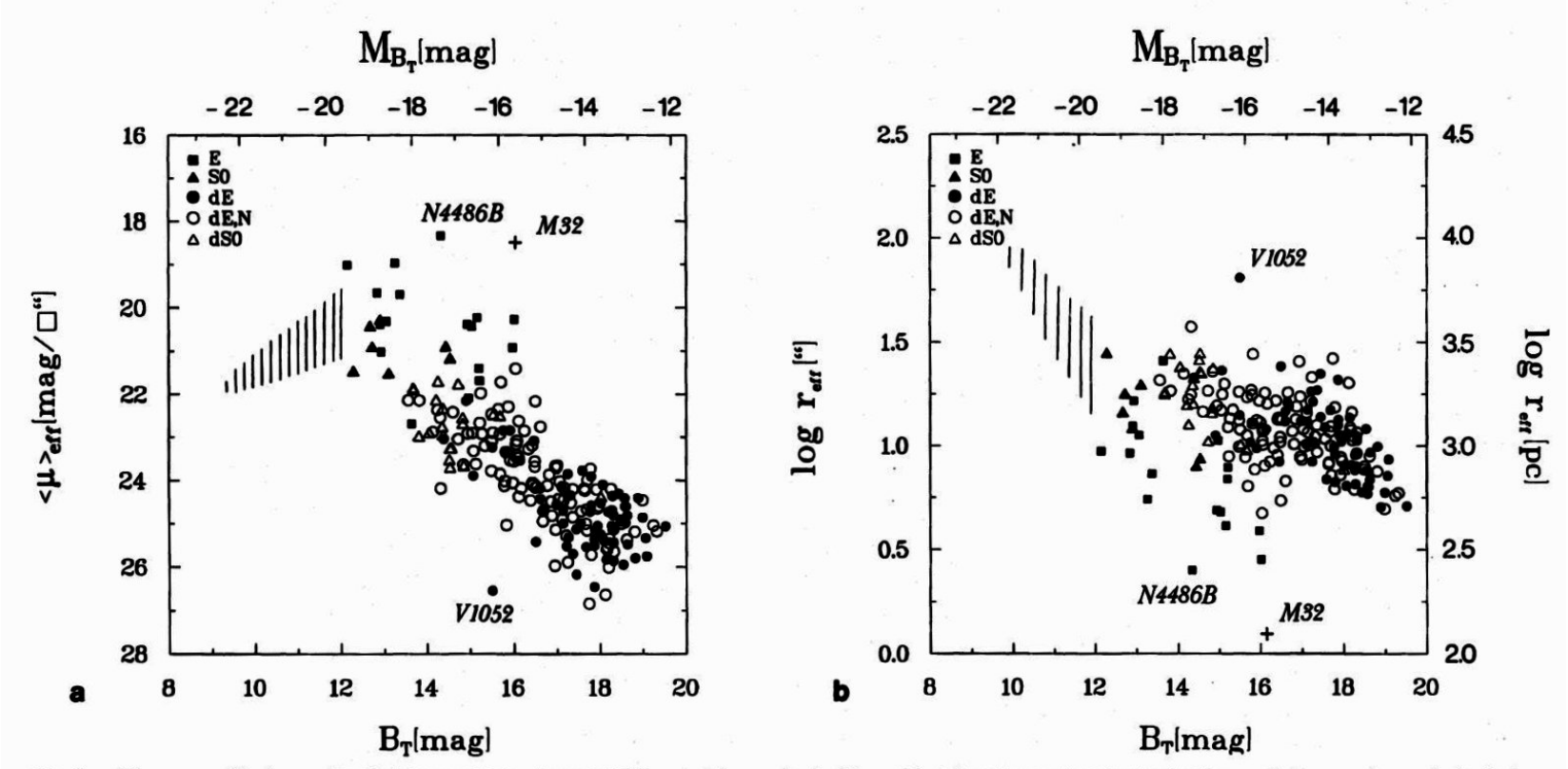

Fig. 1. **a** The mean effective surface brightness ($\langle\mu\rangle_{eff}$ in mag/□") vs. total magnitude (B_T or M_{B_T}) for all sample galaxies, broken up into several morphological classes coded in the figure. The data for a sample of giant E galaxies (shaded area), and for the Andromeda satellite M 32 are added from BST 84. Another compact satellite, NGC 4486 B, and the brightest "iceberg" galaxy, VCC 1952, are indicated. **b** The same as Fig. 1 a but plotting the mean effective radius (log r_{eff}, in arcsec) instead of $\langle\mu\rangle_{eff}$, which is equivalent

Virgo cluster dE (Binggeli, Cameron (1991) *A&A*, **252**, 27)

2. **Dwarf irregulars (dIrr)**:

- brightness distribution in U,B,V shows knots, which correspond to star formation regions. The brightness distribution in the IR is smoother (corresponding to distribution of old stars) and close to exponential.
- dwarf irregulars again show an ellipticity distribution similar to ellipticals and dwarf ellipticals, but not to spirals ($\Rightarrow$ dwarf irregulars generally are not disk-like).
- the transition from spirals to irregulars is smooth, apparent structures (spiral arms, bars) disappear with decreasing L_B and are replaced by irregular structures.
- the HI gas distribution is often much more extended than the distribution of stars (even more so than in spirals). HI dominates the baryonic mass of faintest objects ($M_{\text{stars}} < M_{\text{gas}}$).
- **Blue Compact Dwarfs**: extreme type of dwarf irregulars with star formation bursts concentrated in one very bright region. Some BCD may be genuinely young objects which form stars for the first time (e.g. II Zw 18).
- star formation in irregulars and BCDs leads to expanding bubbles of HII gas and can cause significant gas loss.

Irregular Dwarf Galaxies (in Virgo cluster):

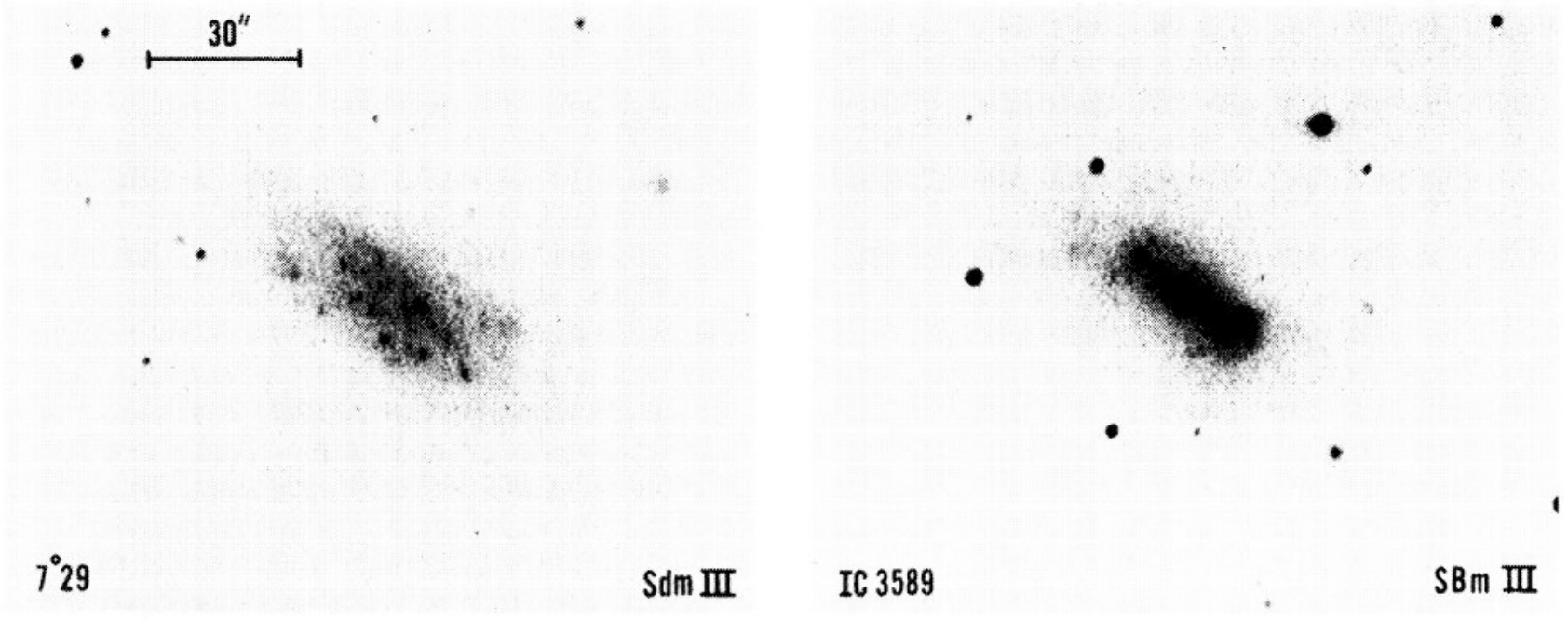

see: Sandage A., Binggeli B. (1984) *AJ*, **89**, 919

Blue Compact Dwarf Galaxies (in Virgo cluster):

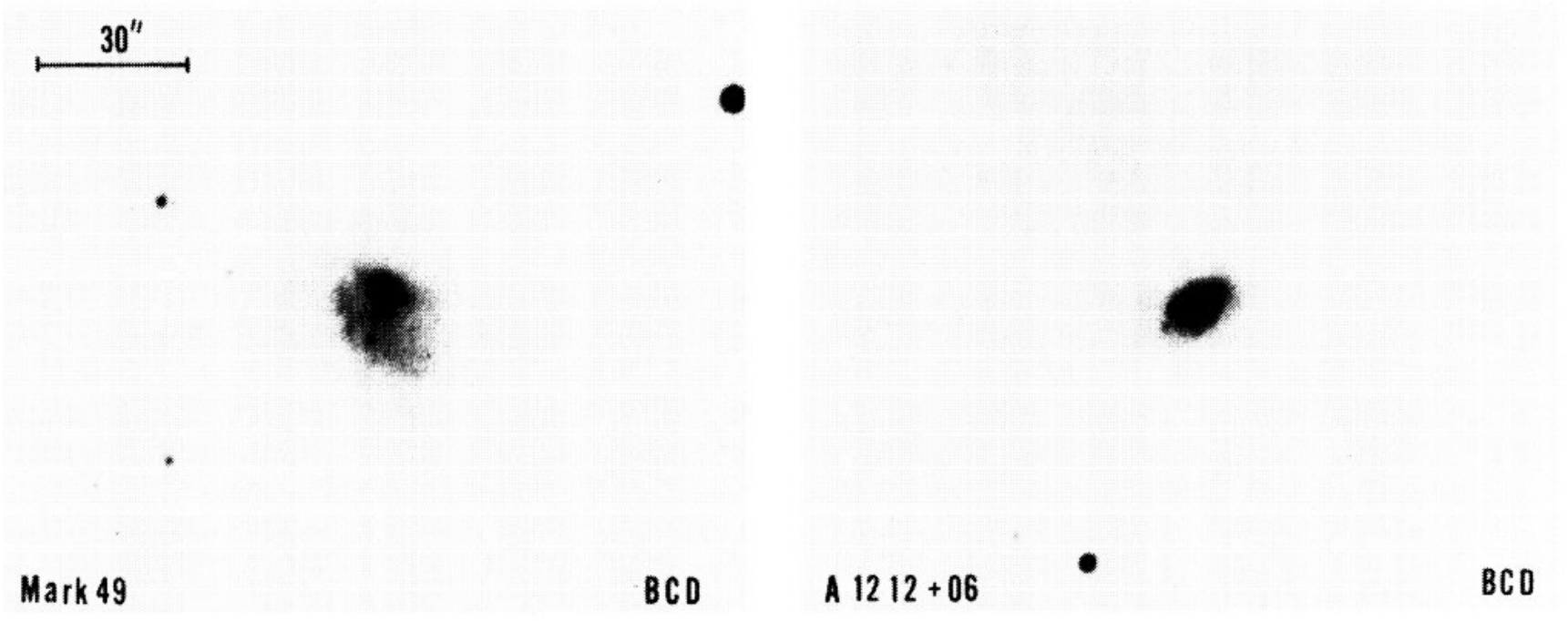

see: Sandage A., Binggeli B. (1984) *AJ*, **89**, 919

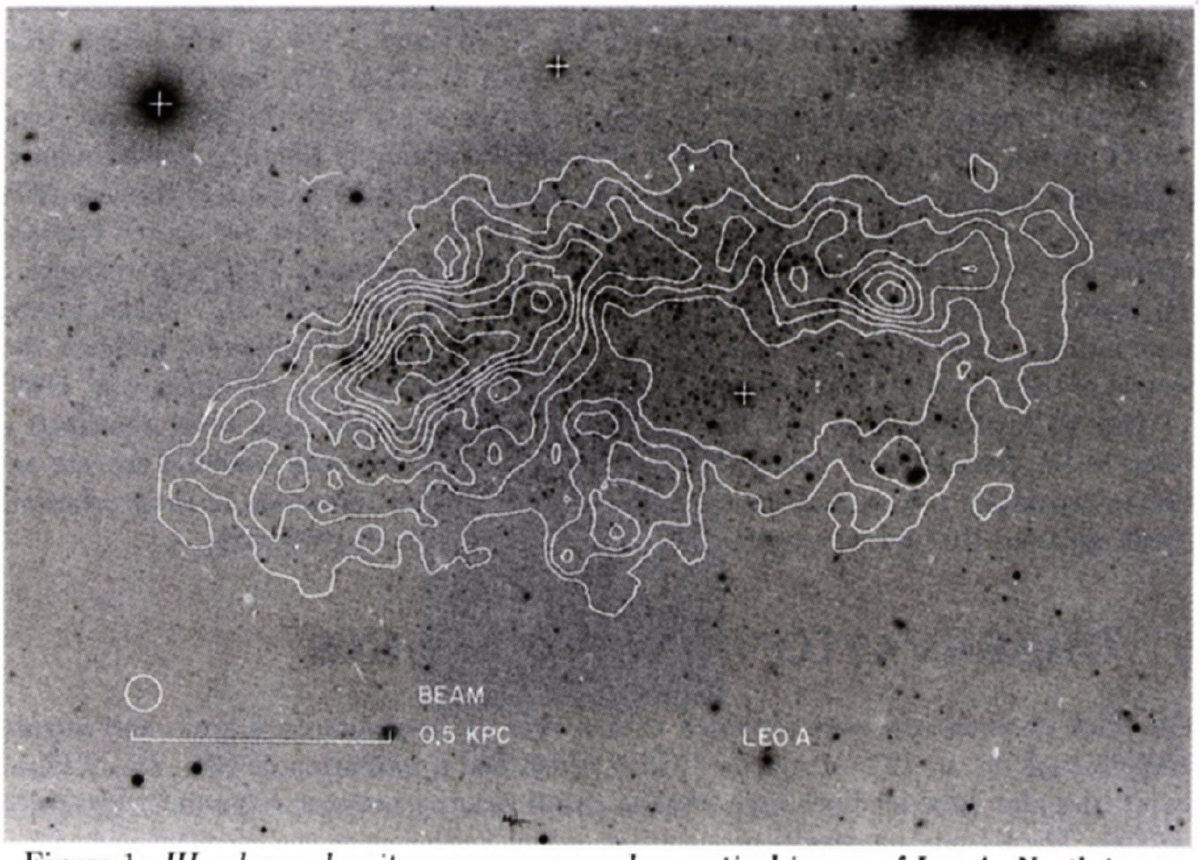

Figure 1: *HI column density map superposed on optical image of Leo A. North is up and East is to the left. The circle represents the 14.5" beam. The contours are at intervals of 10 % of the peak column density of 3.6* $\times 10^{21}$ cm^{-2}.

see: Lo et al. (1994) in *Panchromatic View on Galaxies*

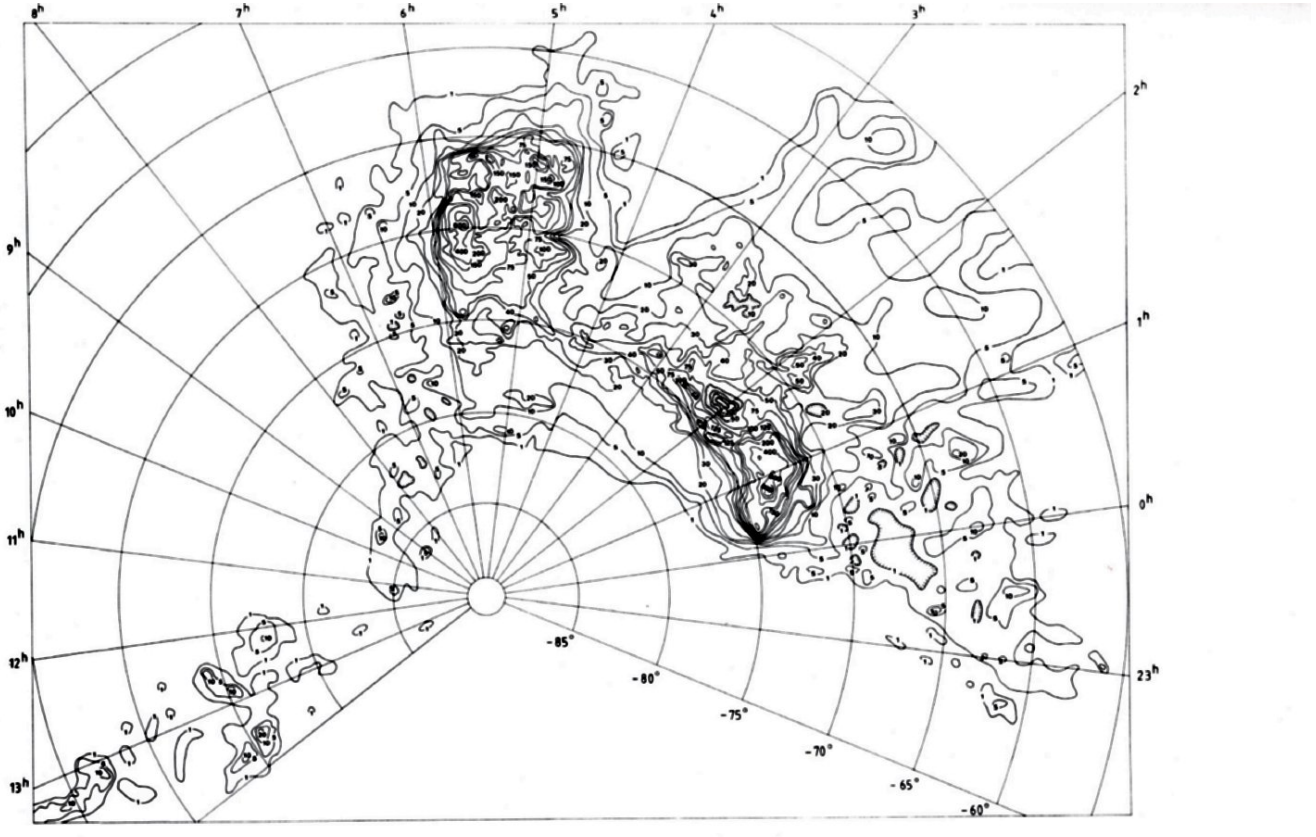

Fig. 2 The integrated HI surface density contours of the region of the LMC and SMC obtained with the 64-m Parkes radiotelescope. The contour unit is 10^{19} atoms cm^{-2}. Data have been taken from Mathewson et al. (1979), Mathewson, Ford and Fisher (1983), McGee and Milton (1966), and Hindman (1967).

see: Mathewson, Ford (1984) *IAU Symp.*, **108**

Wind Driven Outflow:

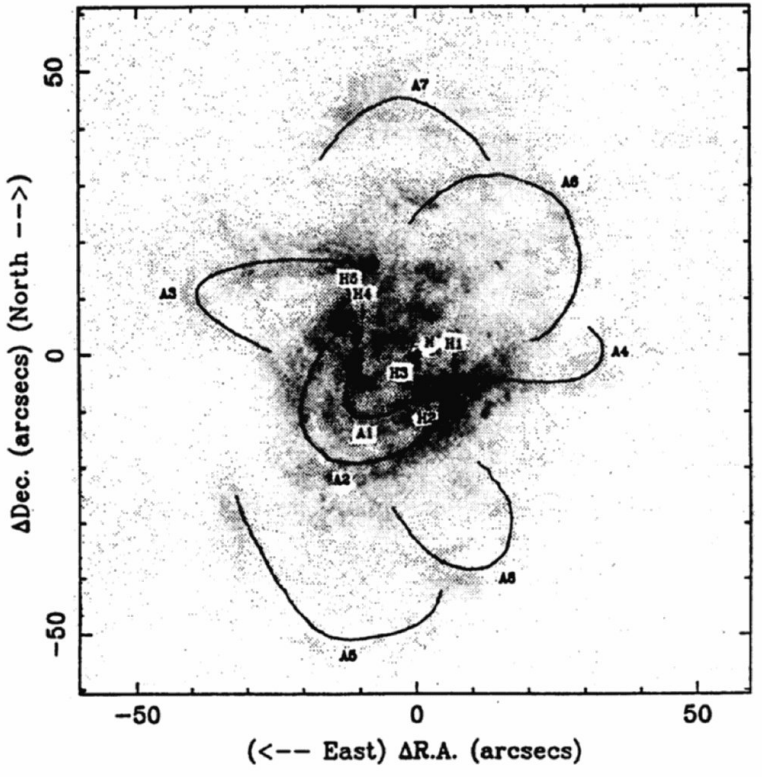

FIG. 12. Identification of H II regions (H) and loops and arcs (A) in the Hα image.

see: Meurer et al. (1992) *AJ*, **103**, 60

6.2 Stellar Populations and Chemistry of Dwarf Galaxies

- Dwarf ellipticals are generally old, i.e. started to form stars ≥ 10 Gyr ago. Some objects may also have had more recent (weaker) episodes of SF, until a few Gyrs ago. These conclusions are mostly based on dwarf companions of the Milky Way that can be resolved into individual stars (see: Hodge (1989) *ARAA*, **27**, 139). Age determinations are more difficult for more distant non-resolved dEs.
- Irregulars usually undergo several bursts of SF (known from the age distribution of stars in the LMC), sometimes separated by long quiescent periods. The oldest stars in the LMC are ≥ 10 Gyr. Fainter objects have fewer bursts ($\rightarrow$ BCDs).

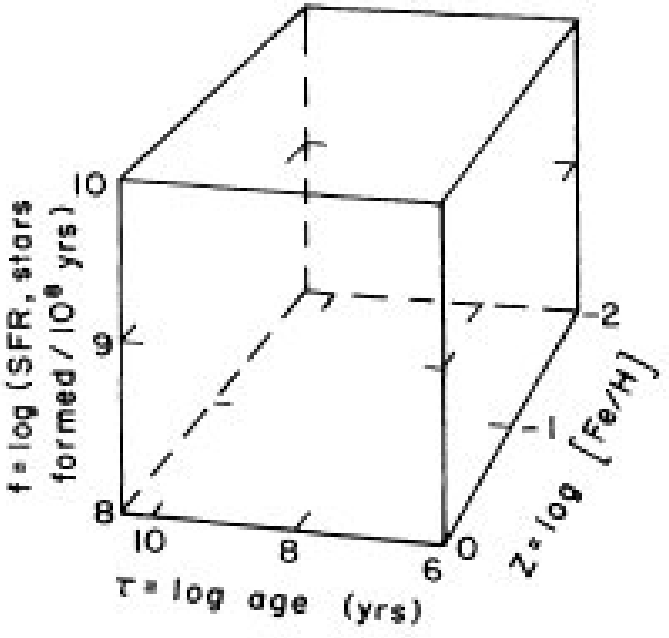

Figure 5 The population box.

History box of star formation and chemical evolution
(see: Hodge (1989) *ARAA*, **27**, 139).

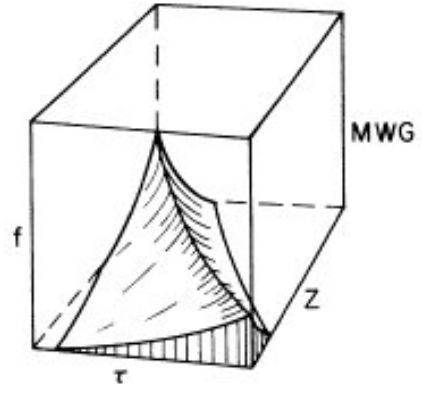

Figure 9 A schematic version of the MWG's volume in the population box.

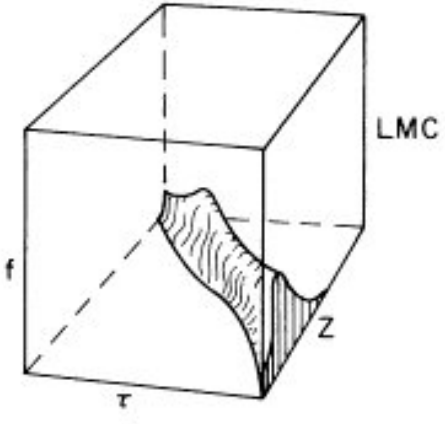

Figure 11 The population history of the Large Magellanic Cloud (LMC).

see: Hodge (1989) *ARAA*, **27**, 139

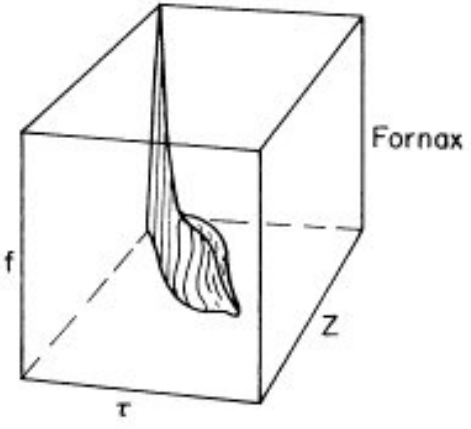

Figure 14 The population history of the Fornax dwarf elliptical.

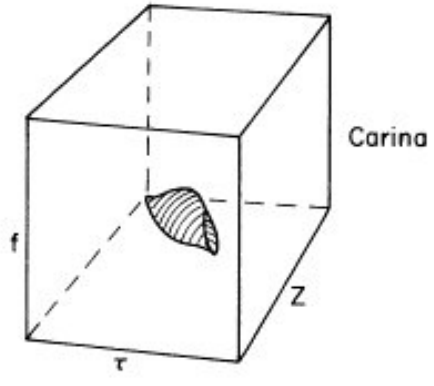

Figure 15 The population history of the Carina dwarf elliptical.

see: Hodge (1989) *ARAA*, **27**, 139

- For dwarfs in the Local Group colour-luminosity diagrams can be derived and the metallicities follow from the colour of the giant branch (GB). Lines represent the GBs of globular clusters with metallicities between 1/3 and 1/100 of solar.

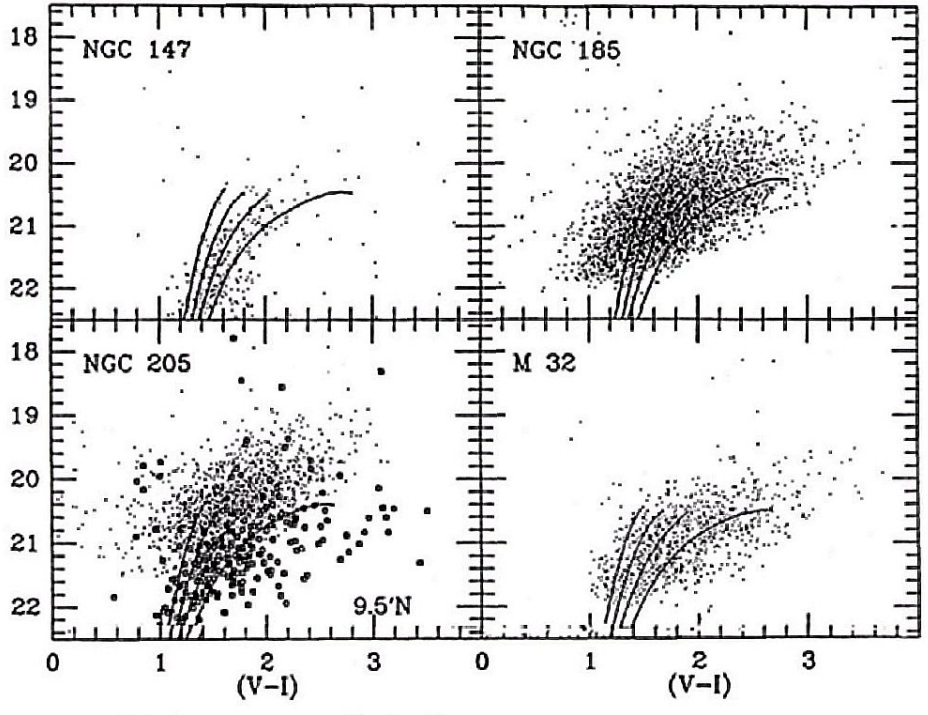

Fig. 1 – I versus $(V\text{-}I)_0$ color-magnitude diagrams.

Freedman (1992) *IAU Symp.*, **149**

- For dwarf ellipticals in general there also exists a good correlation between the Mg_2 index (strength of Mg-absorption at 5170Å) and the velocity dispersion σ ($\rightarrow$ relation between the depth of the potential and the metallicity?).

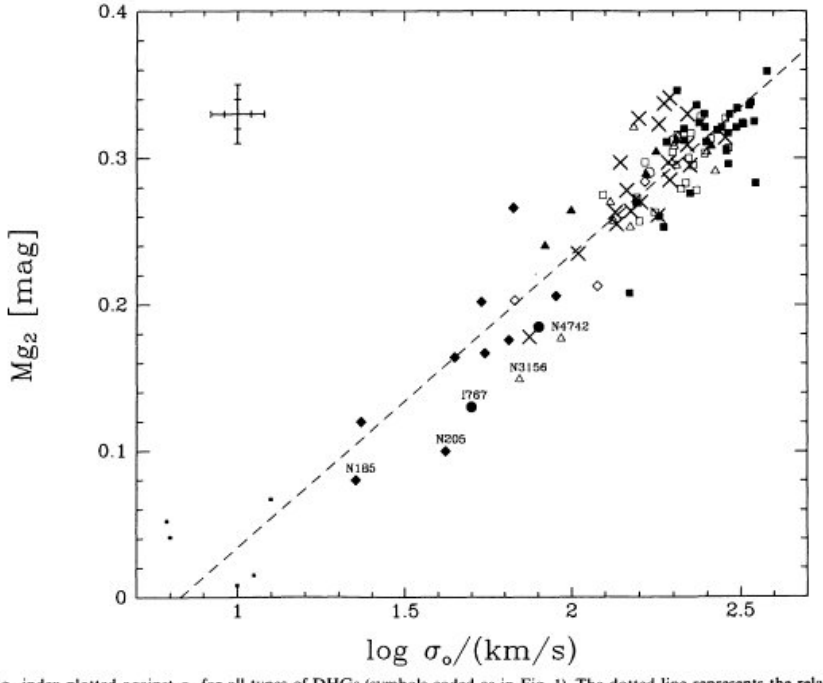

FIG. 3.—Nuclear Mg_2 index plotted against σ_0 for all types of DHGs (symbols coded as in Fig. 1). The dotted line represents the relation $Mg_2 = 0.20 \log \sigma_0 - 0.166$. Galaxies which show evidence for young or intermediate age stars are labeled. Representative error bars are shown in the upper left, the larger error bars refer to the objects with low values of σ_0, the smaller ones to luminous ellipticals and bulges. The Mg_2–log σ_0 correlation is tight over many decades in galaxy size and all DHG types.

Bender (1992) *IAU Symp*, **149**; Bender, Burstein & Faber (1993) *ApJ*, **411**, 153

- The metallicity of dwarf irregulars can be derived from the emission lines of their interstellar medium. There exists a very strong correlation between metallicity and luminosity (Skillman (1989) *ApJ*, **347**, 881).

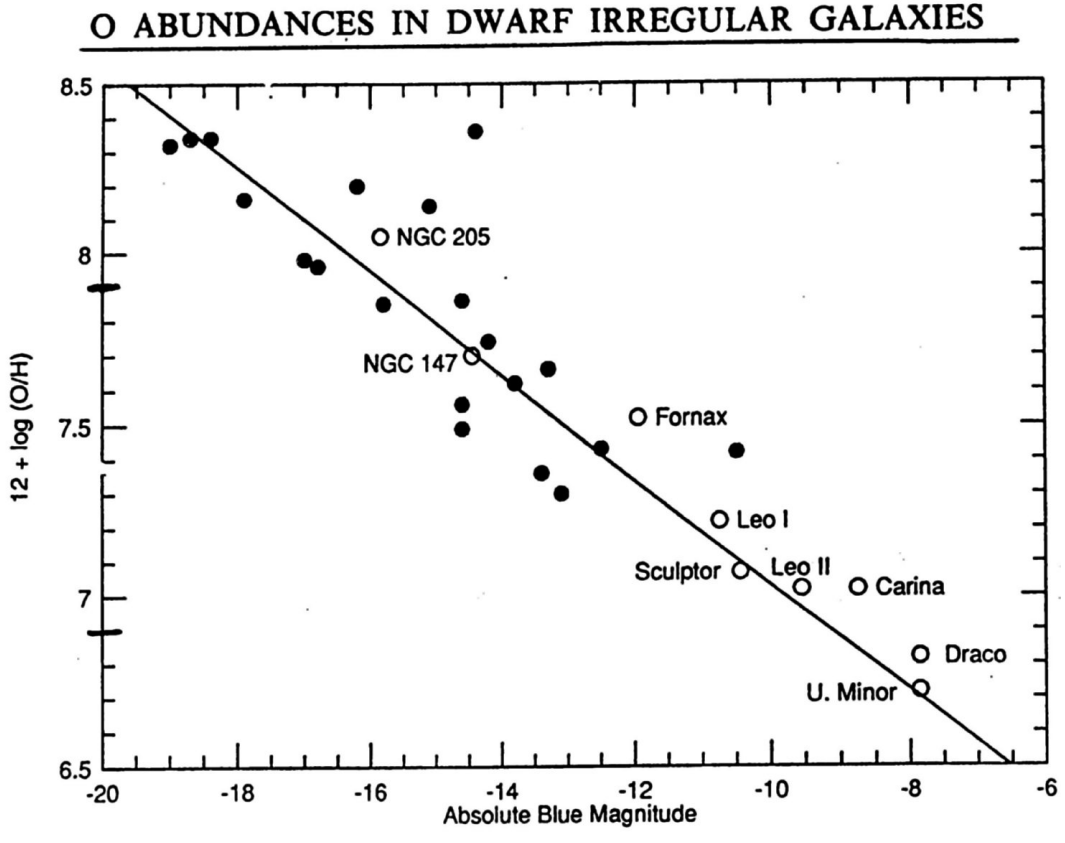

$\Rightarrow$ Both dwarf ellipticals and dwarf irregulars appear to follow a single relation between metallicity and luminosity (or: potential depth/velocity dispersion):

$$Z \propto L_B^{0.4}$$

Interestingly, the gas-to-star ratio does not seem to be very important. Apparently, the metallicity of the stars depends only on the total number of stars produced (luminosity!) and not on the gas mass left at present time.

$\Rightarrow$ The enrichment history must be different from the closed box model! A summary of problems is given by Skillman & Bender (1995) *Rev.Mex.A.A.*, **3**, 25.

6.3 Kinematics of Dwarf Galaxies

- Dwarf elliptical galaxies:
  - follow a similar relation between luminosity and central velocity dispersion as bright elliptical galaxies (see below):

$$L_B \propto \sigma_o^{2.5...3}$$

  - show too little rotation for their flattening and are therefore supported by anisotropic velocity dispersion (however, only few objects were measured so far). The reason for the anisotropy is not yet understood.
  - of very low luminosity ($10^6 - 10^7 L_{B,\odot}$) can have extremely high M/L. Assuming nearly isotropic velocity dispersions, the M/L of dwarf elliptical companions of the Milky Way can be determined by measuring the redshifts of individual stars and using:

$$M \simeq \frac{5}{G} r_e \sigma_0^2$$

($\sigma_0 =$ central velocity dispersion).

Table 4. Properties of dwarf spheroidal galaxies.

Galaxy	M_V	d (kpc)	ϵ	r_c (′)	μ_0 ($\frac{mag}{\square'}$)	$\sigma_{0,p}$ ($\frac{km}{s}$)	$(M/L_V)_0$ ($\frac{M_\odot}{L_{\odot V}}$)	ρ_0 ($M_\odot/pc^3$)	$\rho_{0,L}$	c	$\rho_{min,2}$ ($\frac{M_\odot}{pc^3}$)
Fornax	−12.4	145	0.30	11.3	14.8	10.	5.7	0.073	0.026	0.8	0.004
Sculptor	−11.4	78	0.34	6.2	15.0	7.0	11	0.41	0.076	1.0	0.01:
Carina	−9.2	92	0.31	6.0	16.4	8.8	53	0.50	0.019	0.7	0.03
Draco	−8.9	75	0.29	5.4	16.3	10.5	94	1.3	0.028	0.7	0.09
Ursa Minor	−8.9	69	0.55	6.6	16.4	10.5	83	1.0	0.024	0.4	0.13

ABSTRACT. This review focuses on dark matter in the low-luminosity dwarf spheroidal galaxies that are satellites of our own Galaxy. Originally controversial, the large velocity dispersions in Draco and Ursa Minor are now incontestable and the dispersions of Carina, Sculptor, and Fornax have increased as the data have improved. Mass-to-light ratios from core fitting range from 5.7 for Fornax to 94 for Draco. These values are larger than those found for globular clusters and for most low-luminosity ellipticals, suggesting that all of the dwarf spheroidal satellites of our Galaxy contain dark matter. The presence of non-stellar dark matter in Draco, Ursa Minor, and Carina seems hard to avoid. The data are consistent with all the galaxies having dark halos with a central density of $\sim 0.1\ M_\odot/pc^{-3}$.

see: Pryor C. (1992) in *Morphological and Physical Classification of Galaxies*

The high dispersions in the Draco and Ursa minor dwarfs could also be due to motion in binary stars. However, this has been excluded in long term monitoring of the stars.

$\Rightarrow$ Draco and Ursa minor are everywhere dominated by dark matter!

Table 2. Dwarf spheroidal velocity dispersion studies.

Galaxy	N_s	N_v	σ (km s^{-1})	Instr.	Reference
Draco	23	65	10.5	1	Olszewski (1990)
Ursa Minor	18	41	10.5	1	Olszewski (1990)
Carina	13	27	8.8 ± 2.5	2,3	Seitzer et al., (1990a and pers. comm.)
Sculptor	16	22	6.3 ± 1.2	3	Armandroff and Da Costa (1986)
	7	9	7.2 ± 2.3	1	Aaronson and Olszewski (1987b)
	32	52	7.0 ± 1.2	3	Da Costa and Armandroff (1990)
Fornax	80	80	$9.4^{+1.5}_{-1.4}$	6	Paltoglou and Freeman (1987, 1990)
	30	60	10.5 ± 1.8	2,3	Seitzer et al., (1990b and pers. comm.)
	20	24	10.5	8	Mateo et al., (1990)

see: Pryor C. (1992) in *Morphological and Physical Classification of Galaxies*

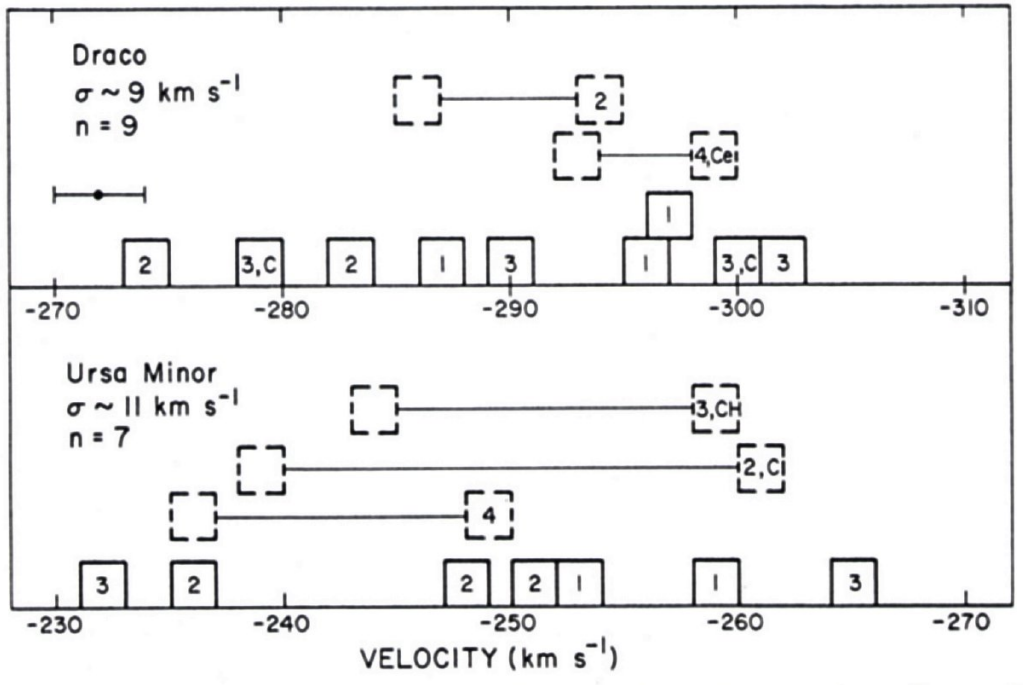

Figure 1. Velocity distributions in two dwarf spheroidals. Quantities inside boxes are the number of epochs a star has been measured. Single boxes represent mean speeds of stars showing no variation larger than the estimated errors, while variables are shown at the extreme range of their measured velocities. C stars are marked.

see: Kormendy J. (1987) *IAU Symp.*, **117**, 153-160

⇒ Do completely dark galaxies exist?

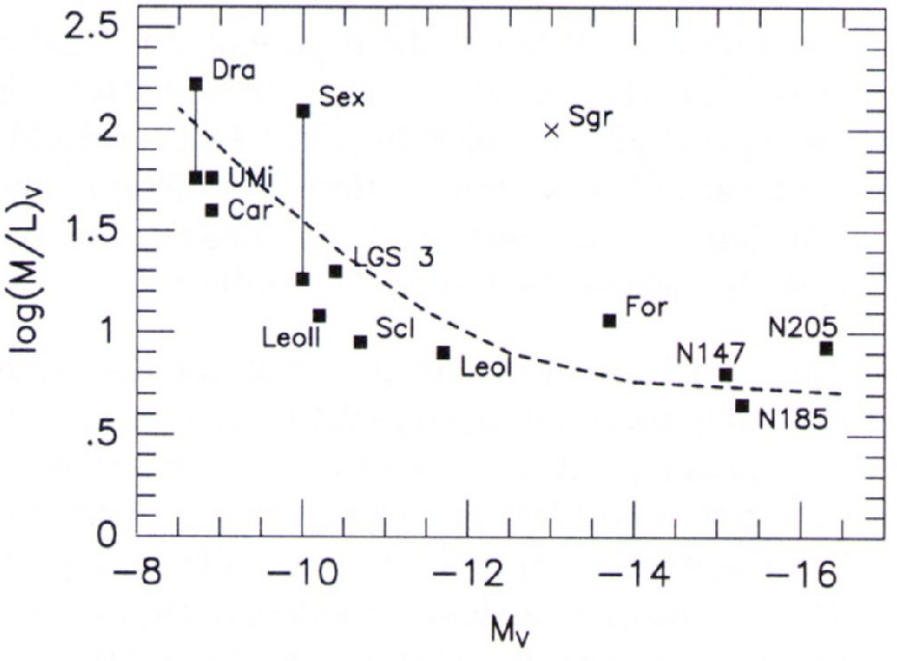

Figure 2. The correlation between M/L_V and M_V for Local Group dSph galaxies with good kinematic data. The dashed line is equivalent to a model where each galaxy has a dark halo mass of $2.5 \times 10^7 M_\odot$ plus a luminous component with $M/L_V = 5.0$. Sagittarius is noted with a cross. The data for the Andromeda dwarfs (apart from LGS 3) come from the references in Mateo 1994.

see: Mateo (1997) *ASP Conf.*, **116**, 266

- Dwarf irregular galaxies:
  - Rotational curves of the HI are now known for a few ten objects, stellar kinematics are almost unknown.
  - The dynamics of the faintest dwarf irregulars is completely dominated by dark matter, also at small radii. The rotation curve and density distribution of the dark matter can therefore be determined directly. It turns out to be consistent with the model for spirals given above. At present, this model is incompatible with the standard non-collisional cold dark matter model.
  - At the same luminosity, dwarf ellipticals and dwarf irregulars have similar rotation velocities and velocity dispersions. For objects dominated by a dark halo everywhere, the following relation between σ_{Halo} and $v_{\text{rot,HI}}$ holds:

$$\sigma_{\text{Halo}} = \frac{v_{\text{circ,Halo}}}{\sqrt{2}} \simeq \frac{v_{\text{rot,HI}}}{\sqrt{2}}$$

Typical values for the central dark matter density and core radii are:

$$r_c \simeq 3\text{kpc}$$
$$\rho_c \simeq 0.05 \frac{M_\odot}{\text{pc}^3}$$

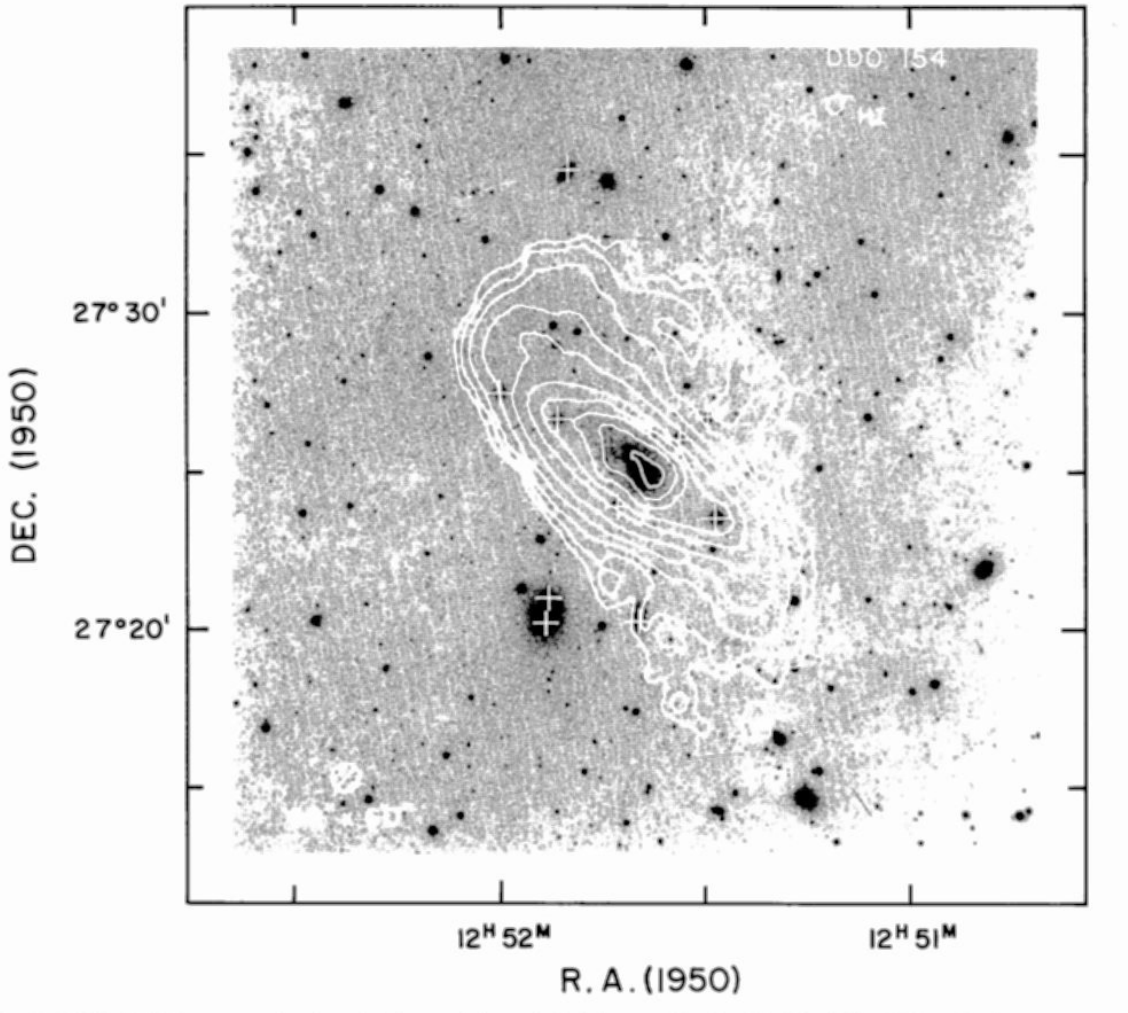

FIG. 2.—The H I distribution superposed on the optical photograph. It was obtained after convolving the original data (35'.3 × 33'.5) to a circular Gaussian beam of 60" (*see bottom left*). The contours are 0.75, 1.5, 3.0, 6, 12, 24, 36, 48, 60, and 72 K.

Dwarf Galaxy DDO 154, negative image = optical, contours = neutral hydrogen (Carignan& Freeman (1988) *ApJ*, **332**, L33)

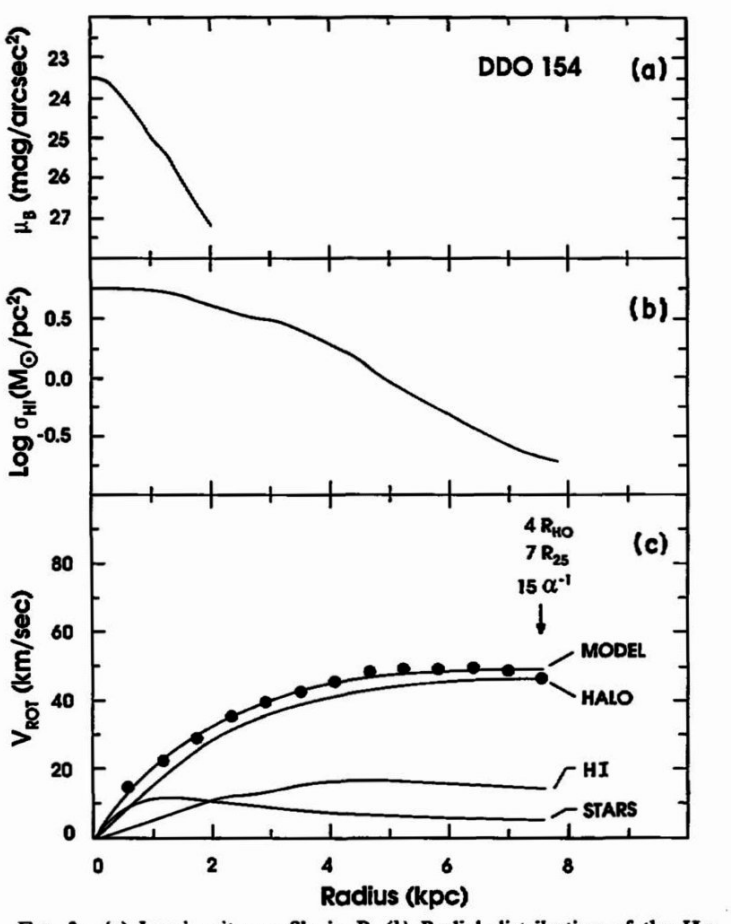

FIG. 3.—(*a*) Luminosity profile in B. (*b*) Radial distribution of the H I surface densities. The central H I surface density is 7.4×10^{20} atoms cm^{-2}. (*c*) Rotation curve and mass model for DDO 154. The errors on the velocities are comparable to the size of the symbols. The stellar disk has $(M/L_B)_* = 1.0$. The dark isothermal halo has a core radius $r_c = 3.0$ kpc and a central density $\rho_0 = 0.016\, M_\odot\, pc^{-3}$.

Dwarf Galaxy DDO 154,
surface brightness profile
of stars and HI,
rotation curve
(Carignan& Freeman (1988)
ApJ, **332**, L33)

TABLE 1

OPTICAL PARAMETERS OF DDO 154 (NGC 4789A)

Parameter	Value
Morphological Type[a]	IB(s)m IV–V
R.A. (1950)[a]	$12^h51^m40^s$
Decl. (1950)[a]	27°25′30″
Galactic extinction,[a] A_B	0.19
Isophotal major diameter,[b] D_{25}	1.′8
Holmberg radius,[b] R_{HO}	1.′5
Axis ratio,[b] b/a	0.57
Inclination[c] ($q_0 = 0.22$), i_c	57.°4
Position angle,[b,c] P.A.	43.°2
Adopted distance	4 Mpc (1′ = 1.16 kpc)
Total B magnitude,[b,d] B_T^0	14.20
Absolute B magnitude, M_T^0	−13.81
Total blue luminosity,[e] L_B	$5.0 \times 10^7\ L_{B\odot}$
Exponential disk parameters:[b]	
Corrected central surface brightness, $B_c(0)$	23.17
Scale length, α^{-1}	(0.5 kpc) 0.′43

[a] De Vaucouleurs, de Vaucouleurs, and Corwin 1976.
[b] Carignan and Beaulieu 1988.
[c] Optical values from the surface photometry.
[d] No correction for internal absorption.
[e] $M_{B\odot} = +5.43$.

Carignan, Freeman (1988) *ApJ*, **332**, L33

TABLE 2

PARAMETERS AND RESULTS FROM THE MASS MODEL

Parameters	Results
Luminous component	$(M/L_B)_* = 1.0 \pm 0.5$
	$M_* = 5.0 \times 10^7\ M_\odot$
	$M_{\rm H\,I} = 2.7 \times 10^8\ M_\odot$
	$(M_{\rm H\,I}/M_*) = 5.4$
Dark halo component	$r_c = 3.0 \pm 0.4$ kpc
	$\sigma = 29.0 \pm 0.3$ km s^{-1}
	$\rho_0 = 0.016\ M_\odot$ pc^{-3}
At last point (7.6 kpc)	$\boxed{(M_{\rm dark}/M_{\rm luminous}) = 12}$
	$M_{\rm dark+luminous} = 4.0 \times 10^9\ M_\odot$
	$\boxed{(M/L_B)_{\rm total} = 80}$

DDO 154, Carignan, Freeman (1988) *ApJ*, **332**, L33

6.4 Neutrino Phase Space Density in Comparison with the Phase Space Density of Dark Matter in Dwarf Galaxies

- Massive neutrinos were believed to be possible candidates for dark matter. As it turns out, relatively strong lower limits on the neutrino masses can be derived from the dark matter densities in dwarf galaxies.

- The phase space density f of neutrinos (leptons) is given by a Fermi-Dirac distribution:

$$f(p) = \frac{2g_\nu}{h^3} \frac{1}{e^{\frac{pc}{kT}} + 1} \tag{6.1}$$

($g_\nu = g_{\text{flavor}} \cdot g_{\text{Spin}}$, the factor 2 results from the anti particles).
The maximum allowed phase space density is reached by neutrinos with $p = 0$:

$$f_{\text{max}} = \frac{g_\nu}{h^3} \tag{6.2}$$

(Note: A more careful argument starts with the highest phase space density for neutrinos during their creation in the cosmological model. This density is lower than the above and preserved during expansion because of Liouville's theorem, that states that the phase space density cannot increase in non-dissipative systems.)

- If the dark matter in dwarf galaxies consists of neutrinos, and if these have a nearly isotropic velocity dispersion, then the phase space density in these galaxies should follow a Maxwellian distribution:

$$f(p) = \frac{n_0}{m_\nu^3 (2\pi\sigma^2)^{3/2}} \, e^{-\frac{p^2}{2m_\nu^2\sigma^2}} \qquad \begin{cases} n_0 = \text{number density} \\ \sigma = \text{velocity dispersion} \\ m_\nu = \text{neutrino mass} \end{cases} \tag{6.3}$$

Again, the maximum density is reached for $p = 0$:

$$f_{\text{max}} = \frac{\rho_0}{m_\nu^4 (2\pi\sigma^2)^{3/2}} \qquad \rho_0 = m_\nu \cdot n_0 \tag{6.4}$$

This must be smaller than f_{max} from equation (6.2):

$$\frac{g_\nu}{h^3} \geq \frac{\rho_0}{m_\nu^4 (2\pi\sigma^2)^{3/2}}$$

Using the relation:

$$\boxed{\rho_0 = \frac{9\sigma^2}{4\pi G r_c^2}}$$

(which is valid for isotropic spherical distributions, see King models in Binney/Tremaine) leads to:

$$\boxed{m_\nu^4 \geq \frac{9h^3}{2(2\pi)^{5/2} g_\nu G \sigma r_c^2}}$$

or:

$$\boxed{m_\nu \geq 101\text{eV} \left(\frac{\sigma}{100\frac{\text{km}}{s}}\right)^{-1/4} \left(\frac{r_c}{1\text{kpc}}\right)^{-1/2} g_\nu^{-1/4}}$$

Inserting the typical observational data for dwarfs given above leads to:

$$\boxed{m_\nu > 200 \text{ eV} g_\nu^{-1/4}}$$

if the dark matter halos of dwarf galaxies are entirely formed by neutrinos.

$\Rightarrow$ **This is in contradiction with the mean neutrino density** $n_\nu = 109 g_\nu cm^{-3}$ **following from big-bang nucleosynthesis and with the observed cosmic density parameter** $\Omega_\nu < 1$**:**

$$\Omega_\nu \leq 1 \quad \Rightarrow \quad m_\nu \leq 55 g_\nu^{-1} eV$$

or:

$$\Omega_\nu \leq 0.2 \quad \Rightarrow \quad m_\nu \leq 11 g_\nu^{-1} eV$$

(Note: The critical density of the universe is $\rho_{\text{crit}} \simeq 10^{-29} g\, cm^{-3} = 5930\, eV\, cm^{-3}$)